Search for an math xmlns="http://www.w3.org/1998/Math/MathML">mi>s/mi> /math>-wave resonance in math xmlns="http://www.w3.org/1998/Math/MathML">mmultiscripts>mi>Li/mi>mprescripts>/mprescripts>none>/none>mn>7/mn>/mmultiscripts>/math> just above the proton-decay threshold

N. Dronchi, J. Berkman, R. J. Charity, J. M. Elson, L. G. Sobotka, A. G. Thomas, A. Saastamoinen, M. Barbui, J. Bishop, C. E. Parker, B. T. Roeder, G. V. Rogachev, D. P. Scriven, S. T. Marley, and R. M. Shaffer

Phys. Rev. C **107**, L061303 — Published 20 June 2023

DOI: 10.1103/PhysRevC.107.L061303

Search for an s-wave resonance in ^{7}Li just above the proton decay threshold

N. Dronchi,[1,*] J. Berkman,[2] R.J. Charity,[2] J.M. Elson,[2] L.G. Sobotka,[1,2] A.G. Thomas,[2] A. Saastamoinen,[3] M. Barbui,[3] J. Bishop,[3] C.E. Parker,[3] B.T. Roeder,[3] G.V. Rogachev,[3,4,5] D.P. Scriven,[3,4] S.T. Marley,[6] and R.M. Shaffer[6]

[1]*Department of Physics, Washington University, St. Louis, Missouri 63130, USA*
[2]*Department of Chemistry, Washington University, St. Louis, Missouri 63130, USA*
[3]*Cyclotron Institute, Texas A&M University, College Station, TX 77843, USA*
[4]*Department of Physics and Astronomy, Texas A&M University, College Station, TX 77843, USA*
[5]*Nuclear Solutions Institute, TAMU 3366 College Station, TX 77843-3366, USA*
[6]*Department of Physics and Astronomy, Louisiana State University, Baton Rouge, Louisiana 70803, USA*

(Dated: June 6, 2023)

Near-threshold resonances play an important role in nucleosynthesis and applied nuclear science. The study of nuclei removed from stability has greatly extended the list of resonances close to decay thresholds. The No Core Shell Model with Continuum (NCSMC) recently predicted an s-wave resonance just above the proton-decay threshold of ^{7}Li at an excitation energy of 10.2 MeV. This potential case of a near-threshold resonance is dependent on the quantum mechanics of the p+^{6}He fragments extended into the continuum. The ^{6}He(d,n)^{7}Li* reaction was employed in an attempt to populate this resonance and search for its proton decay via the invariant-mass method. No evidence of this resonance was found. However, the data collected in this search lead to better constraints on the energy and width of the Isobaric Analog State with (J^π,T) = ($3/2^-$, 3/2) and revealed a new weak resonance just above the IAS in energy, predicted by the NCSMC as a (J^π,T) = ($3/2^-$, 1/2) state and is potentially a part of the anti-analog structure.

I. INTRODUCTION

Resonances near particle-decay thresholds support and facilitate important processes in nucleosynthesis and applied nuclear science. A famous example is the Hoyle state in ^{12}C, being just 287 keV above the α+^{8}Be threshold and 379 keV above the α+α+α threshold; the presence of this state enables the triple-alpha process [1, 2]. In the helium-burning phase of stars, resonant capture through the Hoyle state enhances the rate of carbon production by several orders of magnitude, kick-starting the nucleosynthetic pathway towards elements required for life. A second famous example is the $1/2^+$ resonance in ^{17}O just a few keV above the α+^{13}C threshold but well above the n+^{16}O threshold [3]. This level is an important contribution to the ^{13}C(α,n)^{16}O astrophysical S-factor at low energies [4], one of two reactions in stars that provide the neutron flux for s-process nucleosynthesis.

What is the origin of these near-threshold resonances? For the states mentioned in ^{12}C and ^{17}O, an anthropic argument can be offered to rationalize their existence [5]. If they didn't exist or their properties were different, we might not be here to observe them. If one wishes to know about the true quantum-mechanical origin of a state, they can turn to an *ab initio* calculation such as the No Core Shell Model with Continuum [6]. *Ab initio* methods are important in calculating properties of light nuclei, as they start from the nucleon-nucleon interaction and build up properties of the many-body system.

Recently, the NCSMC method was used to predict a resonance in ^{7}Li just above the p+^{6}He threshold [7]. The NCSMC combines the No Core Shell Model (NCSM) [8] built on a two-nucleon interaction with the addition of eigenstates from specific mass partitions. The inclusion of scattering mass partitions makes the NCSMC well-suited to describe unbound resonances and clustering structure. The predicted resonance mentioned above, discussed in Vorabbi et al. [7] Sec. III.B and later in this paper Sec. III, is s-wave in nature ($J=1/2^+$) with E^*=10.2 MeV and Γ=130 keV. Such a state would be the lowest-energy positive-parity state in ^{7}Li. This prediction motivates the experiment presented in the present work as a test of the predictive capabilities of the NCSMC method.

II. EXPERIMENTAL METHODS

This experiment was performed at the Texas A&M University Cyclotron Institute with a primary ^{7}Li beam produced using the K150 cyclotron. The ^{7}Li(d,^{3}He)^{6}He reaction along with the Momentum Achromat Recoil Spectrometer (MARS) were used to produce a ^{6}He secondary beam at 6.4 MeV/nucleon with 75% purity (25% ^{3}H contaminant) [9]. The beam intensity, monitored by a 1-inch-diameter plastic scintillator at zero degrees, varied through the experiment between 1-8$\times10^4$ pps. The momentum acceptance of MARS was $\pm$1.2% with a beam spot approximately 10 mm in diameter at the target. The ^{6}He beam impinged on a secondary 2.65 mg/cm^2 CD_2 target, and the ^{6}He(d,n) reaction produced excited states of ^{7}Li.

Charged particles were detected and identified using an array of four ΔE-E [Si-Si] telescopes, a setup previously employed to study ^{10}C [10]. Each quadrant had

* n.dronchi@wustl.edu

TABLE I. Comparison between the TUNL evaluations [13, 14] and the current measurements for states in ^{6,7}Li and ^{8}Be. Uncertainties on the measured values represent the statistical uncertainty of the fit.

		Evaluated [13, 14]		Measured	
Nuclei	state	E* (MeV)	Γ (keV)	E* (MeV)[a]	Γ (keV)
^{6}Li	3^+	2.186(2)	24(2)	2.187	- [b]
^{7}Li	$7/2^+$	4.652	69	4.643(1)	92(4)
^{8}Be	0^+, g.s.	0	5.5×10^{-3}	0.0017(3)	0.004(1)
	1_1^+	17.640(1)	10.7(5)	17.646(2)	15(4)
	1_2^+	18.150(4)	138(6)	18.170(10)	158(27)

[a] Invariant masses are measured and then shifted by the ground state energies of the AME2020 mass evaluations [15].
[b] Fixed

two layers of Si from the HIRA array [11]: a 65-μm-thick ΔE single-sided Si detector with 32 strips, backed by a 1.5-mm-thick Si double-sided E detector with 32×32 strips. Both layers were 6.4 × 6.4 cm in area with quadrants arranged with an offset from the center to produce a 1.6-cm-square hole for the unreacted beam to pass through. A circular beam blocker with $\varnothing_{inner}$=1.6 cm and $\varnothing_{outer}$=3.8 cm was used to protect the inner portions of the Si detectors from elastic scattering. The detector array was located 23.5 cm downstream from the the target, a distance that optimizes the detection of the low p+^{6}He relative energies of the predicted resonance. The angular range spanned lab angles from θ=5° to 20°. Readout of the Si-strip information was performed with HINP16C chips, requiring a coincidence between a ΔE and E detector to record data [12].

The ΔE and E silicon detectors were calibrated with a ^{226}Ra alpha source with five peaks between 4.784 and 7.686 MeV. A high-energy calibration point was obtained using elastic scattering of ^{7}Li on a Au target at 38.6 MeV. "Punch-through" protons, with an energy higher than 15.5 MeV and a range approaching 1.5mm in Si, were gated out of the data. A gate on the relative time between the ΔE and E pairs was applied to each particle identification as well as a requirement that the the strips spatially match.

The particle-unbound excited states of light nuclei around ^{7}Li were studied using the invariant-mass method, where correlations between decay fragments are reconstructed to give the parent excitation energy [16]. Selected, well known, states in ^{6,7}Li and ^{8}Be were used to confirm the calibration as well as constrain simulations (see latter for detail). These calibration resonances are shown in Fig. 1 with fit values summarized in Table I. The intense ^{6}Li ($J^\pi=3^+$) resonance, shown in Fig. 1(a), was checked to be consistent across all decay angles to ensure the transverse decays perpendicular to the beam axis (primarily dependent on position information) and longitudinal decays parallel to the beam axis (primarily dependent on the energy calibration) reconstructed to the same excitation energy.

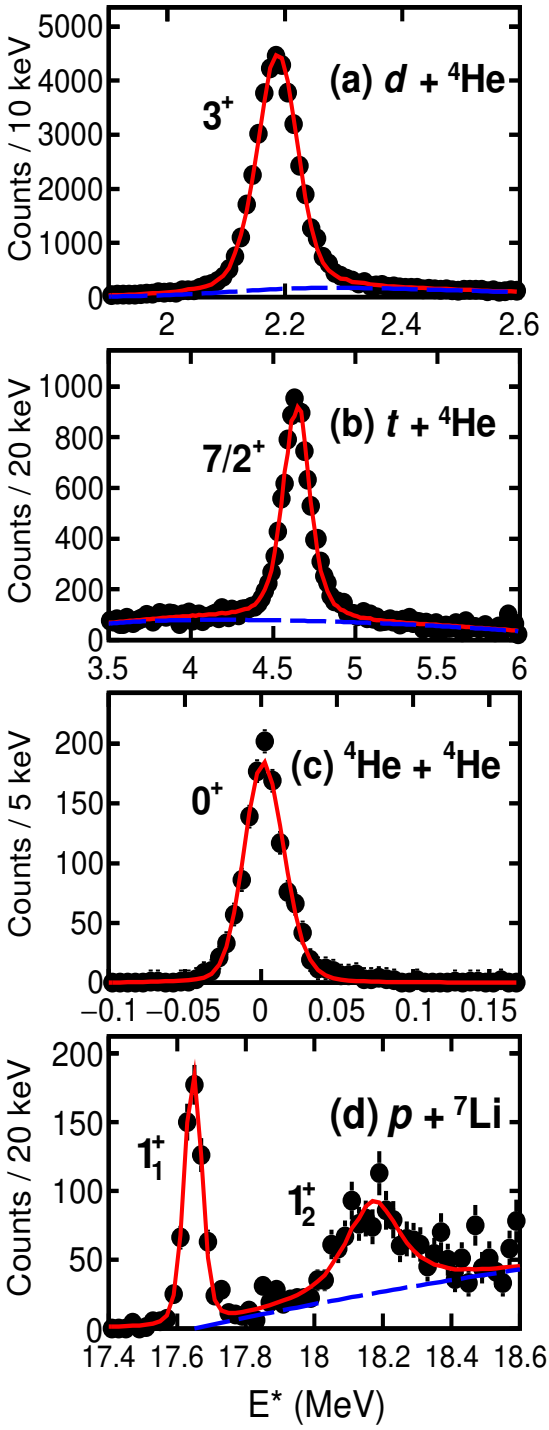

FIG. 1. Efficiency-corrected invariant-mass reconstructions along with simulations fitted to determine the energy and width for: (a) ^{6}Li (3^+) from charge exchange of the ^{6}He beam, (b) inelastically excited ^{7}Li ($7/2^-$) from a primary ^{7}Li beam on the CD_2 target, (c)(d) near-threshold states ^{8}Be (g.s.), ^{8}Be (1_1^+), and ^{8}Be from proton pickup on a primary ^{7}Li beam. In each fit, the red solid line indicates the total fit with the background component indicated by a blue dashed line.

III. EXPERIMENTAL RESULTS

The efficiency-corrected excitation-energy spectrum of ^{7}Li from detected p+^{6}He fragments is shown in Fig. 2. This figure shows the total fit (red solid line) with two resonances (green dotted lines) and a linear background (blue dashed line). The first and most prominent resonance observed is at E_1^*=11.295(10) MeV, Γ_1=184(13) keV and is the Isobaric Analog state (IAS) with (J^π,T) = ($3/2^-$, 3/2) [17]. This high-resolution experiment also revealed a high-energy shoulder to the IAS indicating a previously unreported state at E_2^*=11.66(4) MeV, Γ_2=320(90) keV.

Peaks were assumed to have Breit-Wigner intrinsic line shapes with the experimental resolution and efficiency included via a Monte Carlo simulation taking into account the geometry, energy deposition, and energy thresholds [16]. Realistic beam properties such as momentum distribution and beam size and were also included in the sampling. The simulation used energy deposition determined per particle based on energy losses calculated from the SRIM software package [18] while the thresholds were taken from the experiment. Simulation parameters for scattering angle and energy resolution were tuned to fit the energy and width of the ^{6}Li (3^+) state for both longitudinal and transverse decays relative to the beam line. Plots of the relative fragment angle vs. decay energy from the simulation match the background distribution seen in the data. The telescope geometry was located at a large distance from the target to optimize the detection efficiency for low p+^{6}He relative energies while sacrificing the efficiency at high energies. The simulated ^{7}Li→p+^{6}He efficiency is shown (gray dashed line) in Fig. 2.

The fitted parameters for the IAS of E_1^*=11.295(10) MeV, Γ_1=184(13) keV are an update to the evaluated energy and width of E_{IAS}^*=11.24(30) MeV, Γ_{IAS}=260(35) keV [13]. The 10 keV uncertainty assigned to the measured energy of the IAS is a systematic uncertainty assessed by comparing the evaluated and measured energies in Table I; for example, the ^{7}Li ($7/2^-$) state was measured to be 9 keV lower than the evaluated energy. The statistical error here is small compared to this systematic uncertainty. The uncertainty on the reported width is kept as a statistical uncertainty. For the previously unobserved state at E_2^*=11.66(4) MeV, with Γ_2=320(90) keV, the uncertainty represents the correlated statistical uncertainties that dominate. The broader evaluated width for the IAS may have been a result of this broad unresolved second state at E_2^*.

Using the NCSMC method, the near-threshold resonance in ^{7}Li at E^*=10.2 MeV was predicted as a positive-parity proton s-wave resonance with (J^π,T) = ($1/2^+$, 1/2) [7]. A sharp increase in phase shift in the p+^{6}He scattering with an intrinsic width of Γ=130 keV was a robust prediction from this implementation of the NCSMC with a note that this state could have implications to the astrophysical S-factor in the ^{6}He(p,γ)^{7}Li radiative-capture reaction [7]. An estimate of the cross section for such a state was calculated using FRESCO [19], a general purpose reaction code. For both observed states, optical-model parameters for the d+^{6}He entrance channel and p+^{6}He exit channel were taken from d+^{6}Li scattering [20] and p+^{6}Li scattering [21]. The differential cross sections resulting from FRESCO were used in the simulation of the efficiency.

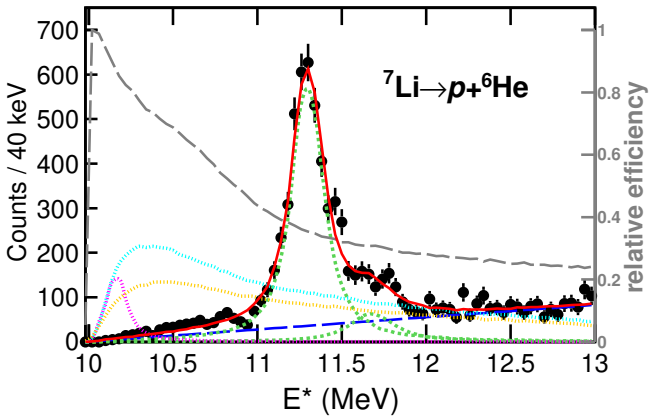

FIG. 2. Efficiency-corrected and fitted excitation-energy spectrum for ^{7}Li→p+^{6}He. The dotted lines represent the simulated resonances where the blue dashed line is a linear background. The magenta finely-dotted peak (not included in the fit) represents the predicted $1/2^+$ state with Breit-Wigner line shape and a small spectroscopic factor (C^2S = 0.02). The sharply rising and slowly decaying cyan and orange finely-dotted lines are two-channel R-matrix line shapes (including n and p decay channels). The cyan (orange) line corresponds to a resonance energy at E^*=10.2 (10.04) MeV. The detector efficiency is overlaid in a grey dashed line with a separate axis on the right. The thresholds for the p+^{6}He and n+^{6}Li (0^+,1) channels are at E^*=9.975 MeV and E^*=10.813 MeV, respectively.

To check for consistency, the yield of the IAS was studied. The cross section for the IAS was calculated using a spectroscopic factor of 0.199 obtained in the p-shell model space with the CKPOT Hamiltonian [22] using the code Oxbash [23]. As most IAS decays are to the open n+^{6}Li (0^+,1) channel, the predicted cross section of the IAS peak was reduced by the proton branching ratio of 0.35 calculated in a two-channel R-matrix approximation with resonance parameters constrained to the measured values. The deduced cross section of the IAS peak, using the number of incident beam particles measured with the plastic scintillator at zero degrees and adjusted for the spectroscopic factor and branching ratio, was found to be consistent with the FRESCO cross section.

Simulation of the proposed $1/2^+$ state (magenta finely-dotted line in Fig. 2), with no neutron branch but with a tiny spectroscopic strength of only C^2S = 0.02, is shown in Fig. 2. The observed yield is far less than even this and in fact no evidence of a narrow state at 10.2 MeV is

seen at all.

Line shapes obtained from two-channel R-matrix calculations [24] were also considered to see the effect of some n+^{6}Li strength in the wave function. The neutron reduced width was set to be 10% of the proton value with the latter set equal to the Wigner limit [25]. The inclusion of the small strength for the n+^{6}Li channel makes the width of the state quite wide and the p+^{6}He line shape has a very long tail. The final p+^{6}He line shape was further modified by scaling with the excitation-energy dependence of the FRESCO predictions for the resonance yield. Predictions with a spectroscopic factor of 0.9 in FRESCO and for R-matrix resonant energies of 10.2 MeV and 10.04 MeV, are also shown in Fig. 2 by the finely-dotted cyan and orange lines respectively. Adding the n+^{6}Li channel allows proton penetration through the high-energy tail of a wider resonance and, as a consequence, the proton branching ratio is only weakly affected by decreasing resonance energy. In both of the two-channel cases considered, one expects to observe a sharp increase in the p+^{6}He yield near the threshold followed by a long decreasing tail. As these features are not observed, these data also exclude a resonance with energy from just above the proton threshold to that of the IAS (11.3 MeV), unless the neutron reduced width exceeds the proton reduced width.

IV. CONCLUSION

This experiment shows no evidence for a s-wave resonance in ^{7}Li just above the p+^{6}He decay threshold. As our experiment was sensitive to both narrow and sharply rising but broad proton resonances, the latter expectation from two-channel R-matrix calculations, we can exclude any state with energy between the proton threshold and the IAS with large proton spectroscopic strength. While a state could exist in this energy region that primarily decays through the n+^{6}Li or ^{4}He+d+n channels, it is not clear how such a state is related to the predicted narrow proton resonance just above the proton threshold.

The theory work that predicted this state mentions three issues in the calculations which could explain why this state might not exist [7]. First, the calculation only includes two-body interactions while the structure of this state is in the three-body ^{4}He+d+n continuum. Perhaps there is an analogy to the structure of ^{6}He, which is thought of as a halo nucleus consisting of a ^{4}He core and two valance neutrons. This suggests a three-body treatment [26]. Another potential problem is that the mass partitions are not coupled. A calculation including the coupling of the open two-body mass partitions might provide an explanation of why we did not observe this resonance, should it exist. The final potential issue is that the calculations only use a two-nucleon chiral interaction where a chiral three-nucleon interaction might yield different results. However, the omission of the three-nucleon interaction is unlikely to erase a resonance that is so conspicuous, being seen in both the n+^{6}Li and p+^{6}He mass partitions, with only the two-nucleon interaction. Unfortunately the likely explanation, the first mentioned above, is also the hardest to test. The resonance might disappear in a calculation that considers the three-body ^{4}He+d+n continuum, an approach the NCSMC is currently unequipped to perform.

The newly observed wide state at E_2^*=11.66(4) MeV might match a different prediction from the NCSMC results, namely a (J^π,T) = ($3/2^-$, 1/2) resonance which is only seen in the p+^{6}He mass partition. This prediction suggests a $P_{3/2}$ resonance at E^*=11.92 MeV with a width of Γ = 410 keV, an overprediction of approximately 260 keV in energy. The IAS was similarly calculated higher in energy by about 420 keV but over-shot the width by a large margin. With a ($3/2^-$, 1/2) spin-parity assignment and an energy near the IAS, this could indicate the observed resonance is a part of the collectivized anti-analog strength, having the same spin and parity as the isobaric analog but with T=1/2 [27].

ACKNOWLEDGMENTS

We acknowledge comments received on a draft version of this work from P. Navrátil and S. Quaglioni. This material is based upon work supported by the U.S. Department of energy, Office of Science, Office of Nuclear Physics under Award No. DE-FG02-87ER-40316 and by the U.S. Department of Energy, National Nuclear Security Administration through the Center for Excellence in Nuclear Training and University Based Research (CENTAUR) under grant No. DE-NA0003841. Additional support at Texas A&M University is provided by the U.S. Department of Energy, Office of Science, Office of Nuclear Science, under Award No. DE-FG02-93ER40773.

[1] F. Hoyle, Astrophys. J. Suppl. Ser. **1**, 12 (1954).
[2] M. Freer and H. Fynbo, Prog. Part. Nucl. Phys. **78**, 1 (2014).
[3] T. Faestermann, P. Mohr, R. Hertenberger, and H.-F. Wirth, Phys. Rev. C **92**, 052802(R) (2015).
[4] S. Cristallo, M. L. Cognata, C. Massimi, A. Best, S. Palmerini, O. Straniero, O. Trippella, M. Busso, G. F. Ciani, F. Mingrone, L. Piersanti, and D. Vescovi, Astrophys. J. **859**, 105 (2018).
[5] E. Epelbaum, H. Krebs, T. A. Lähde, D. Lee, and U. Meißner, Phys. Rev. Lett. **110**, 112502 (2013).
[6] S. Baroni, P. Navrátil, and S. Quaglioni, Phys. Rev. C **87**, 034326 (2013).
[7] M. Vorabbi, P. Navrátil, S. Quaglioni, and G. Hupin, Phys. Rev. C **100**, 024304 (2019).
[8] P. Navrátil, V. G. Gueorguiev, J. P. Vary, W. E. Ormand,

and A. Nogga, Phys. Rev. Lett. **99**, 042501 (2007).
[9] R. Tribble, R. Burch, and C. Gagliardi, Nucl. Instrum. Methods A **285**, 441 (1989).
[10] K. Mercurio, R. J. Charity, R. Shane, L. G. Sobotka, J. M. Elson, M. Famiano, A. H. Wuosmaa, A. Banu, C. Fu, L. Trache, R. E. Tribble, and A. M. Mukhamedzhanov, Phys. Rev. C **78**, 031602(R) (2008).
[11] M. Wallace, M. Famiano, M.-J. van Goethem, A. Rogers, W. Lynch, J. Clifford, F. Delaunay, J. Lee, S. Labostov, M. Mocko, L. Morris, A. Moroni, B. Nett, D. Oostdyk, R. Krishnasamy, M. Tsang, R. de Souza, S. Hudan, L. Sobotka, R. Charity, J. Elson, and G. Engel, Nucl. Instrum. Methods A **583**, 302 (2007).
[12] G. L. Engel, M. Sadasivam, M. Nethi, J. M. Elson, L. G. Sobotka, and R. J. Charity, Nucl. Instrum. Methods A **573**, 418 (2007).
[13] D. Tilley, C. Cheves, J. Godwin, G. Hale, H. Hofmann, J. Kelley, C. Sheu, and H. Weller, Nucl. Phys. A **708**, 3 (2002).
[14] D. Tilley, J. Kelley, J. Godwin, D. Millener, J. Purcell, C. Sheu, and H. Weller, Nucl. Phys. A **745**, 155 (2004).
[15] M. Wang, W. Huang, F. Kondev, G. Audi, and S. Naimi, Chinese Phys. C **45**, 030003 (2021).
[16] R. J. Charity, K. W. Brown, J. Elson, W. Reviol, L. G. Sobotka, W. W. Buhro, Z. Chajecki, W. G. Lynch, J. Manfredi, R. Shane, R. H. Showalter, M. B. Tsang, D. Weisshaar, J. Winkelbauer, S. Bedoor, D. G. McNeel, and A. H. Wuosmaa, Phys. Rev. C **99**, 044304 (2019).
[17] R. J. Charity, S. A. Komarov, L. G. Sobotka, J. Clifford, D. Bazin, A. Gade, J. Lee, S. M. Lukyanov, W. G. Lynch, M. Mocko, S. P. Lobastov, A. M. Rogers, A. Sanetullaev, M. B. Tsang, M. S. Wallace, R. G. T. Zegers, S. Hudan, C. Metelko, M. A. Famiano, A. H. Wuosmaa, and M. J. van Goethem, Phys. Rev. C **78**, 054307 (2008).
[18] J. F. Ziegler, M. Ziegler, and J. Biersack, Nucl. Instrum. Methods A **268**, 1818 (2010).
[19] I. J. Thompson, Computer Phys. Rep. **7**, 167 (1988).
[20] A. Rudchik, A. Budzanowski, E. Koshchy, L. Głowacka, Y. Mashkarov, M. Makowska-Rzeszutko, V. Pirnak, R. Siudak, A. Szczurek, J. Turkiewicz, V. Uleshchenko, and V. Ziman, Nucl. Phys. A **602**, 211 (1996).
[21] L. Elton and A. Swift, Nuclear Physics A **94**, 52 (1967).
[22] S. Cohen and D. Kurath, Nuclear Physics **73**, 1 (1965).
[23] B. A. Brown, A. Etchegoyen, N. S. Godwin, W. D. M. Rae, W. A. Richter, W. E. Ormand, E. K. Warburton, J. S. Winfield, L. Zhao, and C. H. Zimmerman, MSU-NSCL report number 1289.
[24] A. M. Lane and R. G. Thomas, Rev. Mod. Phys. **30**, 257 (1958).
[25] T. Teichmann and E. P. Wigner, Phys. Rev. **87**, 123 (1952).
[26] I. Tanihata, J. Phys. G **22**, 157 (1996).
[27] J. Okołowicz, M. Płoszajczak, R. J. Charity, and L. G. Sobotka, Phys. Rev. C **97**, 044303 (2018).